A mechanistic study of the oxidation of natural antioxidants at the oil/water interface using scanning electrochemical microscopy

Sugihara, Takayasu
Kinoshita, Tomoko
Aoyagi, Shigeo
Tsujino, Yoshio
Osakai, Toshiyuki

(Citation)
Journal of Electroanalytical Chemistry,612(2):241-246

(Issue Date)
2008-01

(Resource Type)
journal article

(Version)
Accepted Manuscript

A mechanistic study of the oxidation of natural antioxidants at the oil/water interface using scanning electrochemical microscopy

Takayasu Sugihara[a,1], Tomoko Kinoshita[b], Shigeo Aoyagi[c], Yoshio Tsujino[a] and Toshiyuki Osakai[b,*]

[a] *Central Research Laboratories, Mandom Corp., 5-12, Juniken-Cho, Chuo, Osaka 540-8530, Japan*

[b] *Department of Chemistry, Graduate School of Science, Kobe University, Nada, Kobe 657-8501, Japan*

[c] *Research & Development Department, Hokuto Denko Co., 3028 Uenohara, Kamiechi, Atsugi-shi, Kanagawa 243-0801, Japan*

[1] Present address: Analysis Technology Research Center, Sumitomo Electric Industries, Ltd., 1-1-3, Shimaya, Konohana-ku, Osaka, 554-0024 Japan.

[*] Corresponding author. Tel./Fax: +81 78 803 5682.

E-mail address: osakai@kobe-u.ac.jp (T. Osakai)

Abstract

Scanning electrochemical microscopy (SECM) was used to study the reaction mechanism of the oxidation of natural antioxidants (ascorbic acid and chlorogenic acid) at oil/water (O/W) interfaces. The apparent first-order rate constants (k_f) were determined for the electron transfer (ET) between the antioxidant in the W phase and the radical cation of 5,10,15,20-tetraphenylporphirinato zinc(II), which was generated on an ultramicroelectrode immersed in the O phase. For both the antioxidants, the values of k_f showed a linear dependence on the square root of the antioxidant concentration in the W phase. The kinetic analysis based on the reaction layer theory suggested a new type of ion transfer (IT) mechanism, in which the ET reaction occurs homogeneously in the O phase (not in the W phase as in the previous IT mechanism).

Keywords: Scanning electrochemical microscopy; Reaction mechanism; Reaction layer theory; Natural antioxidants

Introduction

The polarized oil (O)/water (W) interface could be considered as the simplest model of biomembrane, and the electrochemical study of electron transfer (ET) at the O/W interface seems important for understanding the role of membrane potential in biological ET reactions relevant to respiratory and photosynthetic ET chains and also radical scavenging activities of natural antioxidants.

Since 1979, when Samec et al. [1] first employed cyclic voltammetry to observe an ET reaction between ferrocene in nitrobenzene (NB) and hexacyanoferrate in W, the mechanism of interfacial ET reactions has been a subject of interest. Along with the development of various electrochemical techniques [1–20], it has been recognized that reaction mechanisms of ET at O/W interfaces are classified into two major categories, i.e., the ion-transfer (IT) mechanism and the ET mechanism [21]. The former involves an IT process of the ionic product (or reactant) of a homogeneous ET in one phase (usually, the W phase), and the latter is the "true" heterogeneous ET reaction at the O/W interface. The ferrocene (O)–hexacyanoferrate (W) system, which was studied as the first example of the ET mechanism [1], was actually found to be due to the IT mechanism, where the ET occured "homogeneously" in the W phase and the IT of ferricenium cation as the reaction product was responsible for the current flow through the interface [22–24]. A biomimetic ET system between ascorbic acid (W) and chloranil (O) [22] was also showed to belong to the IT mechanism [25–29]. On the other hand, Geblewicz and Schiffrin [2] first realized a "true" ET, in which a highly hydrophobic organometallic compound (lutetium biphthalocyanine) was used as the

redox species in the O phase. In our recent paper [30], another heterogeneous ET system was realized using 5,10,12,20-tetraphenylporphyrinato cadmium(II) complex and studied by combining several electrochemical techniques, including electron conductor separating oil–water (ECSOW) system [28], digital simulation analysis of cyclic voltammograms [22], and *a.c.* impedance method [31].

Such voltammetric techniques with the polarized O/W interface allow us a detailed understanding of the reaction mechanisms of ET at the O/W interface. However, we often encounter a serious difficulty in studying biomimetic ET systems, which arises from the coupling of ET and IT. For example, regarding the redox reaction between β-nicotinamide adenine dinucleotide (NADH) in W and chloranil or toluquinone in DCE [32], a well-defined polarographic wave for the ET was obtained for chloranil, but not for toluquinone in a definite potential range, where the reduction of toluquinone by NADH was coupled with the proton transfer. In this case, the oxidative product of NADH was confirmed by a bulk electrolysis followed by spectroscopic measurements, however any indication of the ET reaction was not given by the current–potential curve. Similar situations are often encountered, especially in voltammetric studies of biologically relevant redox compounds at O/W interfaces.

Scanning electrochemical microscopy (SECM), which was recently introduced to this field [6-15], is free from the above-mentioned difficulty due to the coupling of ET and IT, since the ET reaction at the O/W interface is detected *indirectly* by means of an ultramicroelectrode (UME) immersed in one phase. In usual SECM measurements, the test O/W interface is not externally polarized, the Galvani potential difference being

usually controlled by addition of a common ion into both phases. Accordingly, SECM measurements can be carried out over a wide range of interfacial potential without the limitation of the potential window. Thus, SECM may be a good approach for the study of interfacial ET reactions for biological compounds, very likely involving the coupling of ET and IT.

In the present paper, we applied SECM to study the mechanisms for the oxidation of natural antioxidants, ascorbic acid (AsA) and chlorogenic acid (CHL), at O/W interfaces. A synergistic antioxidation effect of AsA and α-tocopherol (vitamin E) taking place in biomembranes is well known [33]. In the present SECM measurements, the radical cation of 5,10,15,20-tetraphenylporphirinato zinc(II) ($ZnTPP^{\bullet+}$), which was generated on an UME in the O phase, was used as an analogue of the vitamin E radical for studying the reaction mechanism of the ET reactions with AsA and CHL in the W phase. In a similar manner as vitamin E [33], ZnTPP is oxidized by one electron to form a highly hydrophobic radical cation. SECM studies for the ET reactions between $ZnTPP^{\bullet+}$ and hydrophilic metal complexes at O/W interfaces have been extensively performed by focusing on the driving force dependence of the heterogeneous ET rate constants [6–15]. Although the ZnTPP complex has high hydrophobicity and good redox reversibility, the kinetic data obtained from the SECM measurements for the interfacial ET with AsA and CHL could not be elucidated in terms of a simple, heterogeneous ET mechanism. An analysis based on the reaction layer theory [34,35] has suggested a new type of IT mechanism, in which the ET reaction occurs homogeneously in the O phase, not in the W phase as in the previous IT mechanism.

Recently, a SECM study on the oxidation of AsA by ferrocene at the O/W interface has been reported, though the reaction mechanism remains to be discussed [36].

Experimental

Reagents

ZnTPP was prepared as reported previously [37], and was purified by triple recrystallization from acetone. Tetrahexylammonium perchlorate ($THxClO_4$), which was used as the supporting electrolyte in nitrobenzene (NB) and benzene (BZ), was prepared by equimolar addition of a methanol solution of tetrahexylammonium chloraide (96%, Aldrich) to a methanol solution of sodium perchlorate (98%+, Aldrich); the resulting crude salt was washed five times with deionized water and three times with *n*-hexane, and then triply recrystallized from ethanol–*n*-pentane (2:1). An analytical grade nitrobenzene (99.5%+, Wako) was treated before use with activated alumina for column chromatography (200 mesh, Wako). All other reagents were of the highest grade available and were used as received.

SECM measurements

SECM measurements were performed using the three-electrode electrochemical cell shown in Fig. 1 and all the electrodes were immersed in the upper oil phase (III). The interface between phases (III) and (IV) was the test O/W interface. The interface between phases (II) and (III) was prepared at the end of a glass tube, and phases (I) and (II) was separated by using a hollow gel pellet (BCN; Nisshinbo Industries, Inc.), which was swelled in advance with 1.0 M (= mol dm^{-3}) KCl. The pH of the aqueous phase (IV) was adjusted to 7.0 with a 0.1 M NaH_2PO_4–Na_2HPO_4 buffer. The Ag/AgCl electrode immersed in phase (I) was used as the reference electrode, and the Pt coil in

phase (III) was the counter electrode. A glass-coated Pt-UME (a 10 μm diameter disc-shaped electrode with a 90 μm thick glass sheath) was immersed in phase (III) and used as the working electrode. All electrochemical measurements were performed at air-conditioned room temperature (25 ± 2 ˚C).

The SECM measurements were performed using a scanning electrochemical microscope system (HV-402E, Hokuto Denko Co.) combined with a potentiostat (HA1010mM1A, Hokuto Denko Co.) [38]. To suppress vibrational noises, the electrochemical microscope was set on an air-suspension type vibration isolator (DT-4048M-E, Sigma Koki Co., Ltd.).

The potential difference of the O/W interface ($\Delta_{\mathrm{O}}^{\mathrm{W}}\phi$) was controlled by the concentrations of common ion (ClO_4^-) in the O and W phases. In the presence of the common ion, $\Delta_{\mathrm{O}}^{\mathrm{W}}\phi$ should obey the Nernst equation, being expressed approximately by

$$\Delta_{\mathrm{O}}^{\mathrm{W}}\phi = \Delta_{\mathrm{O}}^{\mathrm{W}}\phi^{\mathrm{o}}_{\mathrm{ClO_4^-}} - \frac{RT}{F}\ln\frac{[\mathrm{ClO_4^-}]}{[\mathrm{ClO_4^-}]_{\mathrm{W}}} \qquad (1)$$

where the bracket denotes the concentration of the indicated species (here, ClO_4^-) in O with no script or in W with the subscript, $\Delta_{\mathrm{O}}^{\mathrm{W}}\phi^{\mathrm{o}}_{\mathrm{ClO_4^-}}$ is the standard ion transfer potential of ClO_4^-, and R, T, and F have their usual meanings. In this study, $[ClO_4^-]$ and $[ClO_4^-]_W$ were kept high by adding 0.25 M $THxAClO_4$ to O and 20 mM $NaClO_4$ to W, in order to avoid the interference from the IT of ClO_4^- in the determination of the ET rate constant.

SECM approach curves

In the SECM measurement, the steady-state UME current (I^k) was monitored by moving the UME tip toward an O/W interface at a constant rate of 1.0 μm s^{-1}. A touch of the UME tip to the interface could be usually detected by a sharp increase or decrease of the current. Using the thus-estimated distance (d) between the UME tip and the interface, the plot of I^k against d, a so-called "approach curve" was obtained. When either the IT of the common ion in both phases or the diffusion of a reactant in the phase where the UME is not immersed is not rate-limiting, the following equations for the approach curve can be used to estimate the apparent first-order rate constant (k_f) for the interfacial ET of the tip-generated species (here, $ZnTPP^{\bullet+}$) [6,12]:

$$I^{k} = \left[\frac{0.78377}{L(1+1/\Lambda)} + \frac{0.68 + 0.3315\exp(-1.0672/L)}{1+F(L,\Lambda)}\right]\left(1 - \frac{I^{ins}}{I^{c}}\right) + I^{ins} \quad (2)$$

$$I^{c} = \frac{0.78377}{L} + 0.3315\exp\left(-\frac{1.0672}{L}\right) + 0.68 \quad (3)$$

$$I^{ins} = \frac{1}{\left[0.15 + \frac{1.5358}{L} + 0.58\exp\left(\frac{-1.14}{L}\right) + 0.0908\exp\left(\frac{L-6.3}{1.017L}\right)\right]} \quad (4)$$

where I^c and I^{ins} represent normalized currents for the diffusion-controlled regeneration of the redox mediator (here, ZnTPP) and no regeneration, respectively; $L = d/a$ (normalized UME–O/W distance), where a is the radius of the UME; $\Lambda = k_f d/D$, where D is the diffusion coefficient of the redox mediator; and $F(L,\Lambda) = (11 + 7.3\Lambda)/[\Lambda(110 - 40L)]$. These currents are normalized by the current at an infinite UME–O/W distance (i.e., the steady-state UME current obtained for the bulk O-phase solution):

$$I_{bulk} = 4nFaDc \quad (5)$$

where c is the bulk concentration of the redox mediator. Note that several coefficients in Eqs. (2)-(4) depend on the configuration of the UME, e.g., the normalized radius of the UME sheath, RG (= r/a, where r is the radius of the whole UME including the electrode and sheath). The above equations can be used for the UME having RG ≥ 10 (for the present UME, RG = 10).

Voltammetric measurements

Fig. 2 shows representative cyclic voltammograms of 0.5 mM ZnTPP at the Pt-UME in BZ and NB. As shown in the figure, a typical steady-state voltammogram, consisting of two well-defined waves, was obtained for either solvent. The two steady-state waves should correspond to the two step-one electron oxidations of ZnTPP [30,39]:

$$\mathrm{ZnTPP} \xrightarrow{-e^-} \mathrm{ZnTPP^{\bullet+}} \xrightarrow{-e^-} \mathrm{ZnTPP^{2+}} \qquad (6)$$

The reversible half-wave potential, or, the formal redox potential for the first redox couple (i.e., ZnTPP/ZnTPP$^{\bullet+}$) was determined to be 0.87 V in BZ and 0.78 V in NB versus the Ag/AgCl reference electrode. The redox potential for the second redox couple (ZnTPP$^{\bullet+}$/ZnTPP^{2+}) was likewise determined to be 1.12 V in BZ and 1.09 V in NB. In the present SECM measurements, the potential applied to the UME was kept at 0.95 V, at which the first one-electron oxidation of ZnTPP should occur at the electrode in either solvent. By applying Eq. (5) for the first limiting current, the diffusion coefficient of ZnTPP in BZ and NB were determined to be 4.38×10^{-6} and 1.55×10^{-6} cm^2 s^{-1}, respectively.

Results and discussion

Fig. 3 shows a set of approach curves, in which normalized currents are plotted against d for the ZnTPP (BZ)/AsA (W) system. The dotted lines are experimental curves, and the solid lines are theoretical curves calculated using Eq. (2). As shown in the figure, the normalized current at shorter distances increased markedly with the concentration of AsA in W. Similar approach curves were obtained for all the systems studied, in which BZ or NB was used as the O phase solvent and AsA or CHL was added as the reductant in W. The current increment at shorter distances clearly showed that $ZnTPP^{\bullet+}$ generated at the UME was reduced by AsA or CHL:

$$ZnTPP \rightarrow ZnTPP^{\bullet+} + e^- \quad \text{(at the UME)} \tag{7}$$

$$ZnTPP^{\bullet+} + e^- \rightarrow ZnTPP \quad \text{(at the O/W interface)} \tag{8}$$

In all the systems, experimental approach curves fit well with the theoretical curves. Then, the apparent first-order rate constants, k_f, was successfully obtained as the fitting parameter for different concentrations of the antioxidant in W. In Fig. 4, the k_f values obtained are plotted on the square root of the concentration of antioxidant in W (denoted by c^W). For all the cases, k_f showed linear dependences on $(c^W)^{1/2}$ in the range up to 0.03 or 0.1 $M^{1/2}$ for the BZ/W and NB/W interfaces, respectively. In the higher concentration ranges, however, the experimental plots deviated downward from the linear plots and approached the measuring limit of the present method. Although the origin of the limit is uncertain, it seems that the good linear plots would provide the values of k_f accurate enough for discussing the mechanism of the interfacial ET

reactions.

Since both AsA and CHL are two-electron reductants, two molecules of $ZnTPP^{\bullet+}$ per molecule of the antioxidant should be reduced. Based on this stoichiometry, three possible reaction mechanisms can be considered, which include one heterogeneous ET mechanism and two homogeneous ET mechanisms. The interfacial two-step ET mechanism, in which k_f should depend linearly on c^W (not on $(c^W)^{1/2}$ in the experiment), has been excluded. Illustrative representations of the three possible mechanisms are shown in Fig. 5. Note that in the figure, the case in which AsA is used as the antioxidant is shown. The validity of the respective reaction mechanism will be discussed below.

For the heterogeneous ET mechanism, the reaction rate of the ZnTPP regeneration, v, is expressed as

$$v = -\frac{\mathrm{d}[\mathrm{ZnTPP}^{\bullet+}]}{\mathrm{d}t} = -k\sqrt{c^{\mathrm{W}}}[\mathrm{ZnTPP}^{\bullet+}] = -k_{\mathrm{f}}[\mathrm{ZnTPP}^{\bullet+}] \qquad (9)$$

where k is the reaction rate constant, which has been set as $k_f = k\sqrt{c^W}$, based on the experimental findings. However, this mechanism stands on the assumption that a pinpoint collision of three reactants occurs just on the O/W interface, which is unlikely because of a kinetic disadvantage.

The second mechanism is due to a homogeneous ET in the W phase, which involves an IT of $ZnTPP^{\bullet+}$ into the W phase. In this mechanism, the IT of $ZnTPP^{\bullet+}$ should precede the homogeneous ET in the W, so the standard ion transfer potential of $ZnTPP^{\bullet+}$ ($\Delta_O^W\phi^\circ_{ZnTPP^{\bullet+}}$) must be in the range where the IT of $ZnTPP^{\bullet+}$ can occur at a

sufficient rate. However, our previous work [30] showed that the radical cation of a metal TPP complex has an excessively low ion transfer potential, thus excluding the possibility of this mechanism.

The third mechanism is due to a homogeneous ET in the O phase, which involves the partition of an antioxidant into the O phase. In this mechanism, the rate of the ZnTPP regeneration can be expressed using the "reaction layer" theory [34,35]:

$$v = -\frac{\mathrm{d}[\mathrm{ZnTPP}^{\bullet+}]}{\mathrm{d}t} = -k_{\mathrm{f}}[\mathrm{ZnTPP}^{\bullet+}] = -\mu k'_{\mathrm{app}}[\mathrm{ZnTPP}^{\bullet+}] \tag{10}$$

where k'_{app} is the apparent rate constant for the ET reaction between the antioxidant and $\mathrm{ZnTPP}^{\bullet+}$ in the reaction layer, and μ the thickness of the reaction layer:

$$\mu = \sqrt{\frac{D_{\mathrm{ZnTPP}^{\bullet+}}}{k'_{\mathrm{app}}}} \tag{11}$$

where $D_{\mathrm{ZnTPP}^{\bullet+}}$ is the diffusion coefficient of $\mathrm{ZnTPP}^{\bullet+}$ in the O phase. If the concentration of antioxidant in the reaction layer is kept constant by rapid distribution of the antioxidant at the interface, k'_{app} can be expressed by

$$k'_{\mathrm{app}} = 2k_1 K_{\mathrm{D}} c^{\mathrm{w}} \tag{12}$$

where k_1 is the bimolecular reaction constant, and K_{D} the partition coefficient of the antioxidant. Here, it is assumed that the ET reaction between the antioxidant and $\mathrm{ZnTPP}^{\bullet+}$ is a "two step-one electron" process in which the first step is the rate limiting step. The k_{f} value is then given from Eqs. (10)–(12) as:

$$k_{\mathrm{f}} = \sqrt{D_{\mathrm{ZnTPP}^{\bullet+}} k'_{\mathrm{app}}} = \sqrt{2D_{\mathrm{ZnTPP}^{\bullet+}} k_1 K_{\mathrm{D}}} \sqrt{c^{\mathrm{w}}} \tag{13}$$

This relation was in accord with the experimental results shown in Fig. 4. Thus, the

third reaction mechanism successfully explained the kinetic data obtained.

Here, let us estimate the bimolecular reaction rate constant (k_1) based on the third mechanism. To determine the K_D values necessary for the estimation, distribution experiments were performed. However, only the K_D value for CHL in the BZ/W system could be obtained ($K_D = 10^{-3.85}$). The values for other systems could not be determined because of the interferences from solvent absorption. Accordingly, K_D was tentatively assumed to be $10^{-4.0}$ to estimate rough values of k_1 for all the systems by using Eq. (13). As shown in Table 1, the estimated k_1 values were in the order of 10^6 to 10^8 M^{-1} s^{-1}. These rate constants are some orders smaller than the diffusion-controlled one (~10^{10} M^{-1} s^{-1}), which is estimated by the Smoluchowski-Debye theory [40, 41].

In the proposed IT mechanism (i.e., mechanism (C) in Fig. 5), the ET reaction occurs homogeneously in the O phase, and hydrophilic product(s) would be partitioned or transferred back into the W phase. In the initial step of the mechanism, only the antioxidant with no charge is partitioned into the O phase. If the antioxidant behaves in the O phase in a similar manner as in W [29], the homogeneous ET of the antioxidant with $ZnTPP^{\bullet+}$ would yield the oxidized form of antioxidant (with no charge) and a proton (H^+) as the reaction products. Though not shown in Fig. 5, the resultant H^+ should be transferred to the W phase, accompanying the transfer of an anionic charge from O to W or the transfer of a cationic charge from W to O. Thus, the present interfacial ET reactions are coupled with the proton-transfer reaction, however the ET mechanisms could be well characterized using SECM without the interference from the proton-transfer reactions.

Conclusions

SECM is useful for studying the reaction mechanism of interfacial ET reactions between $ZnTPP^{\bullet+}$ as an analogue of the vitamin E radical and natural antioxidants such as AsA and CHL. The linear dependence of the apparent ET rate constants on the square root of the antioxidant concentration can be elucidated based on the reaction layer theory with a new type of IT mechanism, in which the ET reaction occurs homogeneously in the O phase. This result seems suggestive in considering the microscopic mechanism of the synergistic antioxidant effect of AsA and vitamin E at biomembranes.

Acknowledgment

We are grateful to Mitsugi Senda, Emeritus Professor of Kyoto University, for his kind suggestion on the use of a reaction layer theory.

References

[1] Z. Samec, V. Marecek, J. Weber, J. Electroanal. Chem. 103 (1979) 11.

[2] G. Geblewicz, D. J. Schiffrin, J. Electroanal. Chem. 244 (1988) 27.

[3] S. Kihara, M. Suzuki, K. Maeda, K. Ogura, M. Matsui, Z. Yoshida, J. Electroanal. Chem. 271 (1989) 107.

[4] Q. Z. Chen, K. Iwamoto, M. Senõ, Electrochim. Acta 36 (1991) 291.

[5] Y. Cheng, D. J. Schiffrin, J. Chem. Soc. Faraday Trans. 89 (1993) 199.

[6] C. Wei, A. J. Bard, M. V. Mirkin, J. Phys. Chem. 99 (1995) 16033.

[7] M. Tsionsky, A. J. Bard, M. V. Mirkin, J. Phys. Chem. 100 (1996) 17881.

[8] M. Tsionsky, A. J. Bard, M. V. Mirkin, J. Am. Chem. Soc. 119 (1997) 10785.

[9] A. L. Barker, P. R. Unwin, S. Amemiya, J. Zhou, A. J. Bard, J. Phys. Chem. B 103 (1999) 7260.

[10] S. Amemiya, Z. Ding, Z. Zhou, A. J. Bard, J. Electroanal. Chem. 483 (2000) 7.

[11] J. Zhang, A. L. Barker, P. R. Unwin, J. Electroanal. Chem. 483 (2000) 95.

[12] M. V. Mirkin, M. Tsionsky in: A. J. Bard, M. V. Mirkin (Eds.), Scanning Electrochemical Microscopy, Marcel Dekker, New York, 2001 (Chapter 8).

[13] Z. Ding, B. M. Quinn, A. J. Bard, J. Phys. Chem. B 105 (2001) 6367.

[14] J. Zhang, P. R. Unwin, Phys. Chem. Chem. Phys. 4 (2002) 3820.

[15] Z. Zhang, Y. Yuan, P. Sun, B. Su, J. Guo, Y. Shao, H. H. Girault, J. Phys. Chem. B 106 (2002) 6713.

[16] B. Quinn, R. Lahtinen, L. Murtomäki, K. Kontturi, Electrochim. Acta 44 (1998) 47.

[17] Z. Ding, D. J. Fermín, P. F. Brevet, H. H. Girault, J. Electroanal, Chem. 458 (1998) 139.

[18] K. Chikama, K. Nakatani, N. Kitamura, Bull. Chem. Soc. Jpn. 71 (1998) 1065.

[19] Z. Samec, in: A. G. Volkov, D. W. Deamer (Eds.), Liquid-Liquid Interfaces, Theory and Methods, CRC Press, Boca Raton, FL, 1996 (Chapter 8).

[20] D. J. Fermín, R. Lahtinen, in: A. G. Volkov (Ed.), Liquid Interfaces in Chemical, Biological, and Pharmaceutical Applications, Marcel Dekker, New York, 2001, pp. 179-227.

[21] T. Osakai, H. Hotta, in: H. Watarai, N. Teramae, T. Sawada (Eds.), Interfacial Nanochemistry, Kluwer/Plenum, New York, 2005 (Chapter 8).

[22] H. Hotta, S. Ichikawa, T. Sugihara, T. Osakai, J. Phys. Chem. B 107 (2003) 9717.

[23] H. Tatsumi, H. Katano, Anal. Sci. 20 (2004) 1613.

[24] H. Tatsumi, H. Katano, J. Electroanal. Chem. 577 (2005) 59.

[25] M. Suzuki, S. Umetani, M. Matsui, S. Kihara, J. Electroanal. Chem. 420 (1997) 119.

[26] T. Osakai, N. Akagi, H. Hotta, J. Ding, S. Sawada, J. Electroanal. Chem. 490 (2000) 85.

[27] T. Osakai, H. Jensen, H. Nagatani, D. J. Fermín, H. H. Girault, J. Electroanal. Chem. 510 (2001) 43.

[28] H. Hotta, N. Akagi, T. Sugihara, S. Ichikawa, T. Osakai, Electrochem. Commun. 4 (2002) 472.

[29] T. Sugihara, H. Hotta, T. Osakai, Bunseki Kagaku 52 (2003) 665.

[30] T. Osakai, S. Ichikawa , H. Hotta, and H. Nagatani, Anal. Sci., 20 (2004) 1567.

[31] T. Osakai, T. Kakutani, M. Senda, Bull. Chem. Soc. Jpn. 57 (1984) 370.

[32] H. Ohde, K. Maeda, Y. Yoshida, S. Kihara, Electrochim. Acta, 44 (1998) 23.

[33] E. Niki, Ann. NY Acad. Sci. 498 (1987) 186.

[34] M. Senda, Rev. Polarogr., 49 (2003) 219.

[35] M. Senda, Rev. Polarogr., 50 (2004) 60.

[36] X. Lu, L. Hu, X. Wang, Electroanalysis, 17 (2005) 953.

[37] A. D. Adler, F. R. Longo, F. Kampas, J. Kim, J. Inorg. Nucl. Chem., 32 (1970) 2443.

[38] S. Aoyagi, M. Matsudaira, T. Suzuki, H. Katano, S. Sawada, H. Hotta, S. Ichikawa, T. Sugihara, T. Osakai, Electrochemistry, 70 (2002) 329.

[39] A. Wolberg, J. Manassen, J. Am. Chem. Soc. 92 (1970) 2982.

[40] M. von Smolchowski, Z. Phys. Chem., 92 (1917) 129.

[41] P. Debye, Trans. Electrochem. Soc., 82 (1942) 265.

Table 1. The reaction rate constants (k_1) for the homogeneous bimolecular ET reactions between $ZnTPP^{\bullet+}$ and antioxidants in O-phase, which were estimated by assuming $K_D = 10^{-4.0}$.

	$k_1/M^{-1}\ s^{-1}$	
	BZ	NB
AsA	6.5×10^8	7.5×10^6
CHL	1.7×10^8	4.9×10^6

Figure Captions

Fig. 1. Schematic representation of the electrochemical cell for SECM measurements. (I) 1.0 M KCl, (II) 20 mM $NaClO_4$, 0.1 M NaCl, (III) 0.5 mM ZnTPP, 0.25 M $THAClO_4$, (IV) 0–10 mM AsA or CHL, 20 mM $NaClO_4$, 0.1 M NaCl, 0.1 M phosphate buffer solution (pH 7.0).WE: working electrode, CE: counter electrode, RE: reference electrode.

Fig. 2. Steady-state cyclic voltammograms for the oxidation of ZnTPP in (A) BZ and (B) NB at a 10 μm-diameter Pt-UME. [ZnTPP] = 0.5 mM. Scan rate: 0.01 V s^{-1}.

Fig. 3. Approach curves for different concentrations of AsA obtained with a 10-μm diameter Pt-UME approaching the BZ/W interface at 1.0 μm s^{-1}. From top to bottom, [AsA] = 10, 1.0, 0.50, 0.25, 0.15, 0 mM. Solid lines: theoretical curves, Circles: experimental values. The theoretical curve at the top represents the diffusion-limited curve for ZnTPP.

Fig. 4. Apparent heterogeneous rate constants (k_f) at (A) BZ/W and (B) NB/W interfaces, which are plotted against the square root of the concentration of antioxidant (AsA or CHL).

Fig. 5. Mechanisms for the oxidation of an antioxidant (AsA or CHL) by $ZnTPP^{\bullet+}$ at O/W interface, which are due to (A) a heterogeneous ET occurring between $ZnTPP^{\bullet+}$ in O and the antioxidant in W, (B) a homogeneous ET occurring in the W phase accompanying the IT of $ZnTPP^{\bullet+}$, and (C) a homogeneous ET occurring in the O phase accompanying the partition of the antioxidant into the O phase. MDA: monodehydro ascorbate, DHA: dehydro ascorbate.

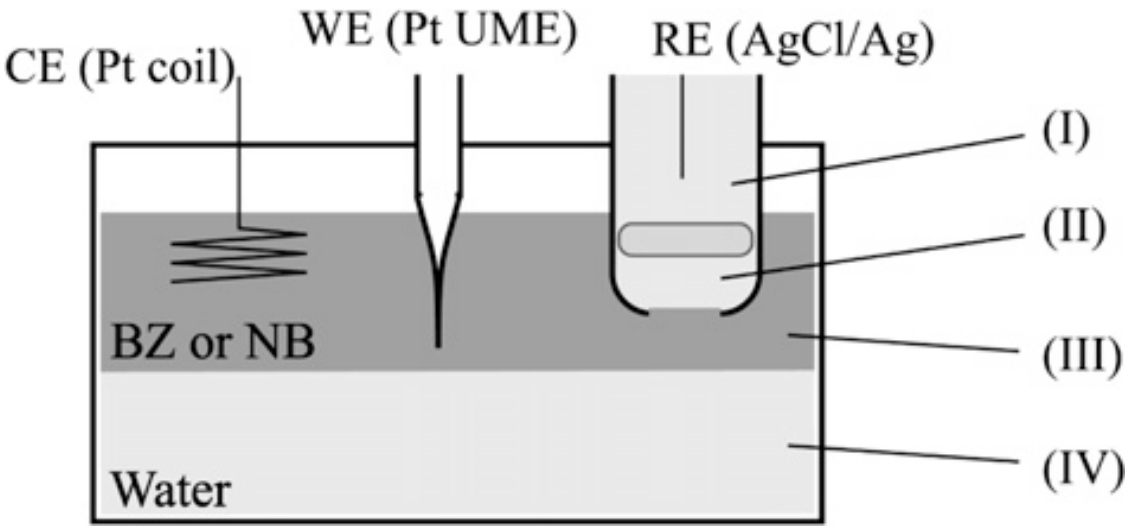

Fig. 1

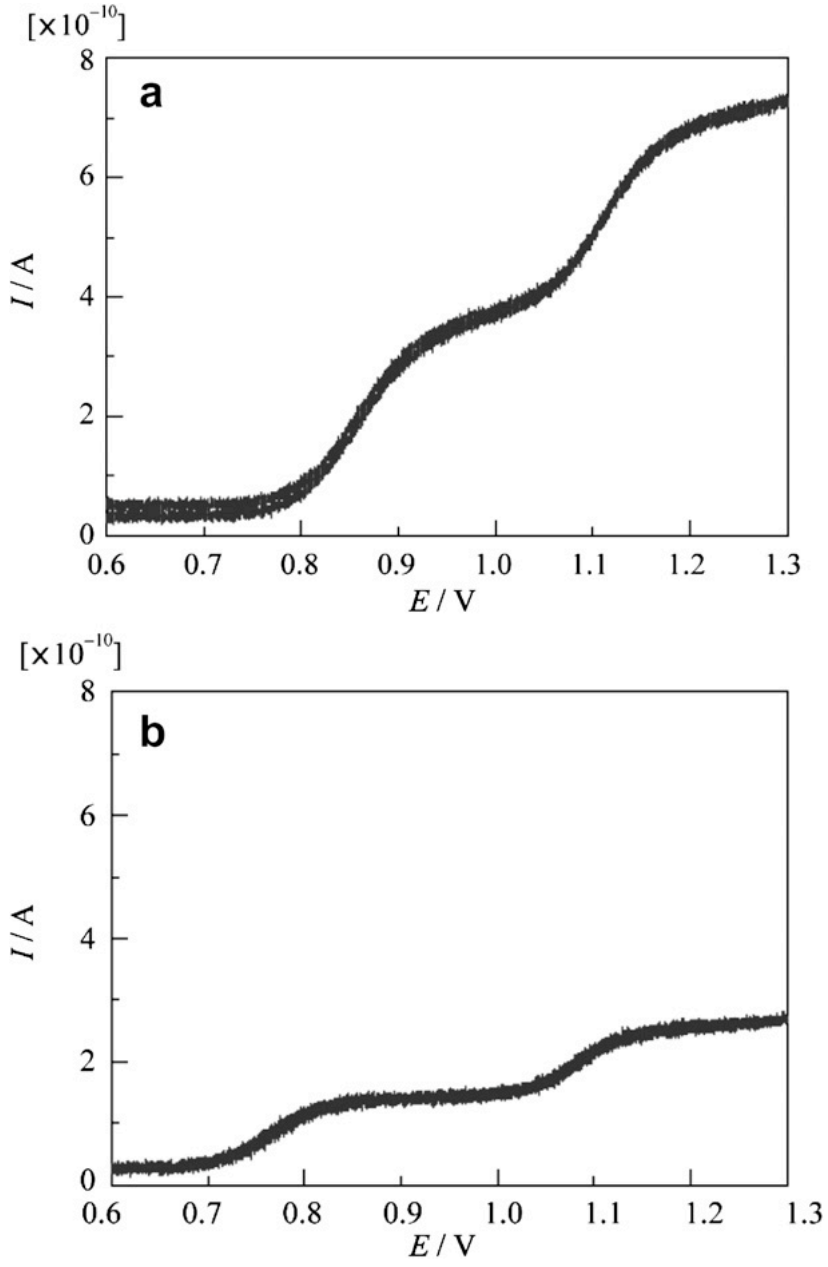

Fig. 2

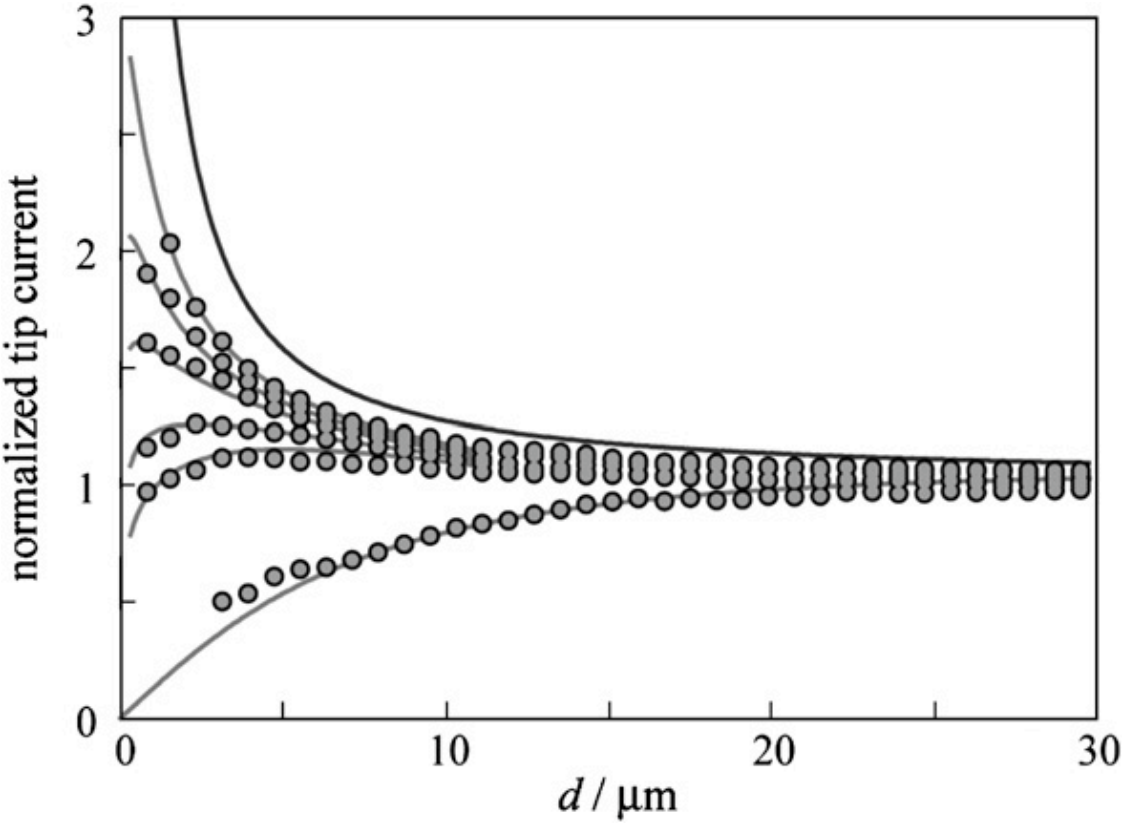

Fig. 3

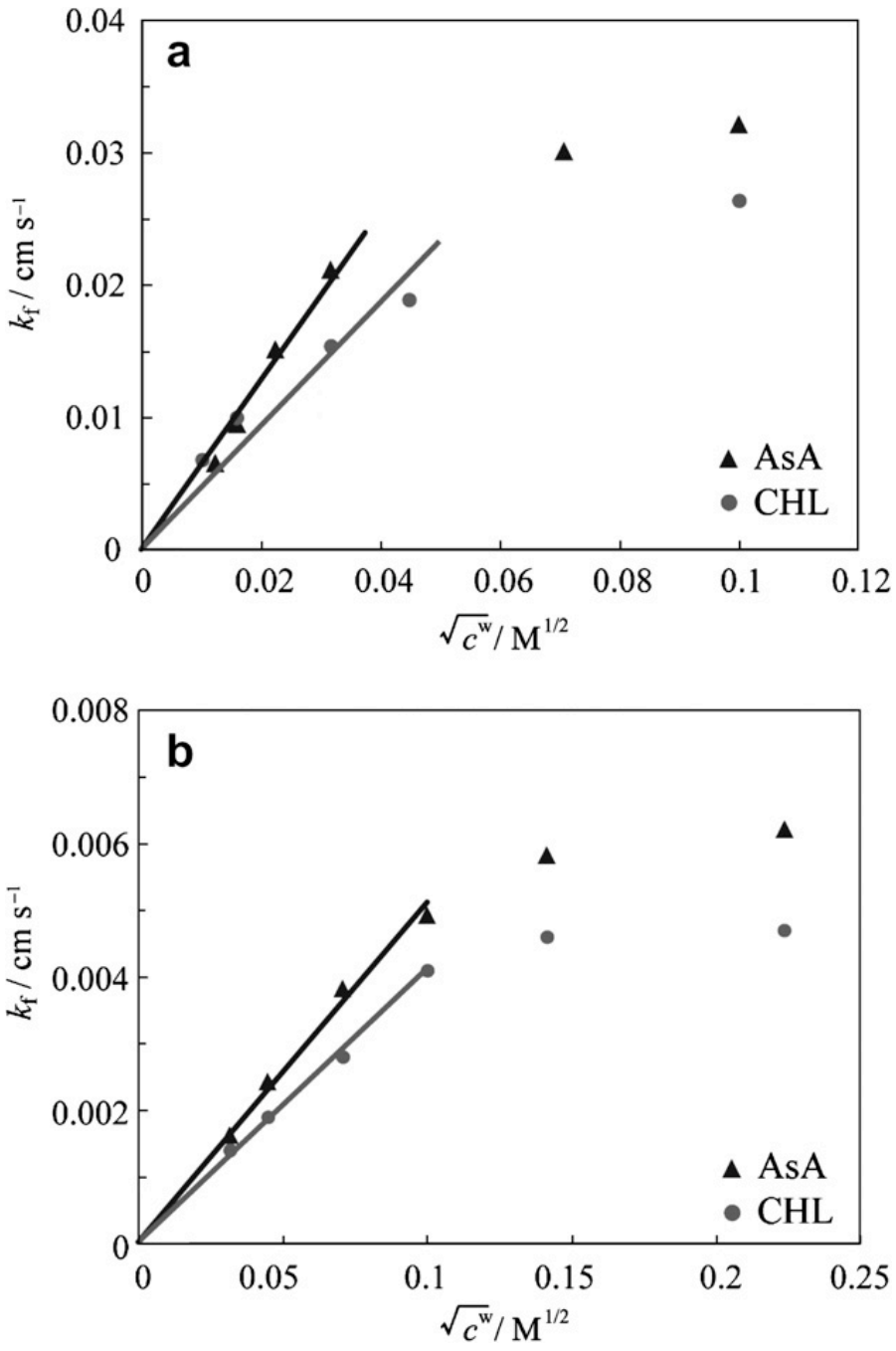
a
0.04
0.03
0.02
0.01
0
k_f / cm s^{-1}
0
0.02
0.04
0.06
0.08
0.1
0.12
$\sqrt{c^w}$ / M$^{1/2}$
AsA
CHL
b
0.008
0.006
0.004
0.002
0
k_f / cm s^{-1}
0
0.05
0.1
0.15
0.2
0.25
$\sqrt{c^w}$ / M$^{1/2}$
AsA
CHL

Fig. 4

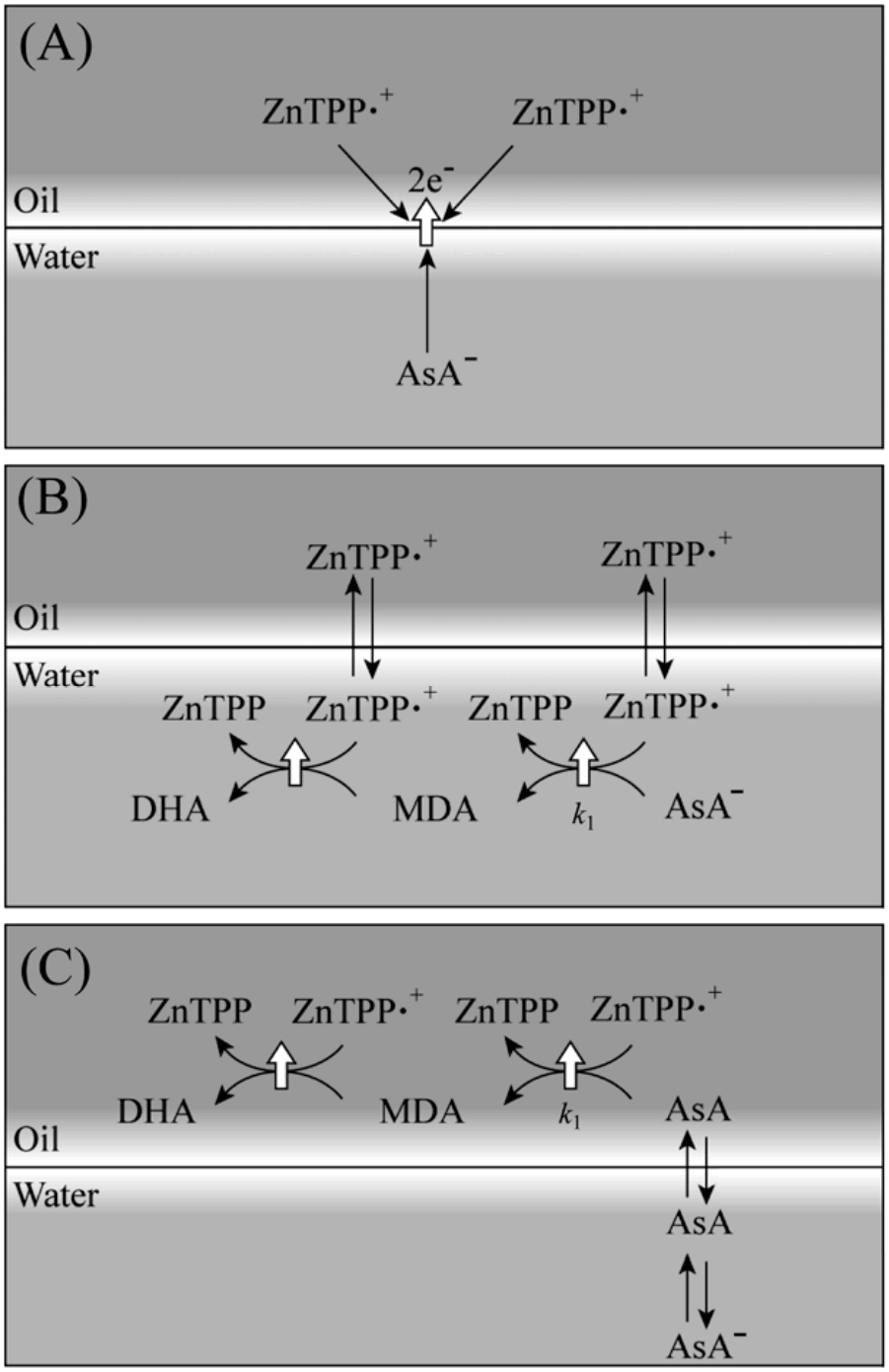
(A)
ZnTPP•+
ZnTPP•+
2e-
Oil
Water
AsA-
(B)
ZnTPP•+
ZnTPP•+
Oil
Water
ZnTPP
ZnTPP•+
ZnTPP
ZnTPP•+
DHA
MDA
k1
AsA-
(C)
ZnTPP
ZnTPP•+
ZnTPP
ZnTPP•+
DHA
MDA
k1
AsA
Oil
Water
AsA
AsA-

Fig. 5